Article

Microcin J25 Has a Threaded Sidechain-to-Backbone Ring Structure and Not a Head-to-Tail Cyclized Backbone

K. Johan Rosengren, Richard J. Clark, Norelle L. Daly, Ulf Gransson, Alun Jones, and David J. Craik

J. Am. Chem. Soc., **2003**, 125 (41), 12464-12474• DOI: 10.1021/ja0367703 • Publication Date (Web): 20 September 2003

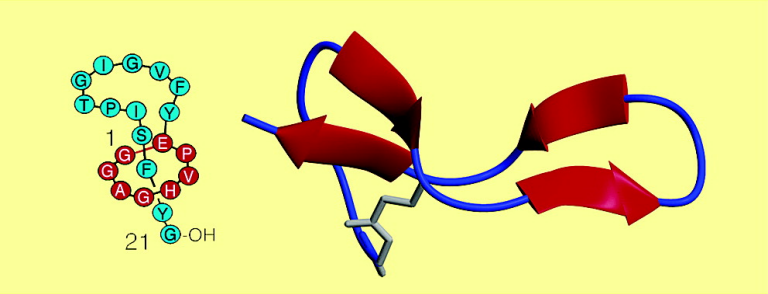

More About This Article

Additional resources and features associated with this article are available within the HTML version:

- Supporting Information
- Links to the 8 articles that cite this article, as of the time of this article download
- Access to high resolution figures
- Links to articles and content related to this article
- Copyright permission to reproduce figures and/or text from this article

View the Full Text HTML

J|A|C|S
ARTICLES
Published on Web 09/20/2003

Microcin J25 Has a Threaded Sidechain-to-Backbone Ring Structure and Not a Head-to-Tail Cyclized Backbone

K. Johan Rosengren, Richard J. Clark, Norelle L. Daly, Ulf Göransson, Alun Jones, and David J. Craik*

Contribution from the Institute for Molecular Bioscience, University of Queensland, Brisbane QLD 4072, Australia

Received June 19, 2003; E-mail: d.craik@imb.uq.edu.au

Abstract: Microcin J25 is a 21 amino acid bacterial peptide that has potent antibacterial activity against Gram-negative bacteria, resulting from its interaction with RNA polymerase. The peptide was previously proposed to have a head-to-tail cyclized peptide backbone and a tight globular structure (Blond, A., Péduzzi, J., Goulard, C., Chiuchiolo, M. J., Barthélémy, M., Prigent, Y., Salomón, R. A., Farías, R. N., Moreno, F. & Rebuffat, S. *Eur. J. Biochem.* **1999**, *259*, 747−755). It exhibits remarkable thermal stability for a peptide of its size lacking disulfide bonds and in part this was previously proposed to derive from its macrocyclic structure. We show here that in fact the peptide does not have a head-to-tail cyclic structure but rather a side chain to backbone cyclization between Glu8 and the N-terminus. This creates an embedded ring that is threaded by the C-terminal tail of the molecule, forming a noose-like feature. The three-dimensional structure deduced from NMR data suggests that slippage of the noose is prevented by two aromatic residues flanking the embedded ring. Unthreading does not occur even when the molecule is enzymatically digested with thermolysin. The new structural interpretation fully accounts for previously reported NMR and biophysical data and is consistent with the remarkable stability of this potent antimicrobial peptide.

Introduction

Although circular proteins were unknown a decade ago, over recent years there have been increasing reports of their discovery in organisms ranging from bacteria to plants and animals.[1] By circular proteins we mean proteins that have a continuous cycle of peptide (amide) bonds in their backbone, as opposed to proteins that are topologically cyclic by virtue of one or more nonpeptidic linkages between backbone segments. For example, there are many proteins that may be regarded as cyclic by virtue of cross-linking disulfide bonds. We also distinguish gene-coded circular proteins from cyclic peptides that have been chemically synthesized or produced enzymatically by peptide synthetases in microorganisms.[2] The latter often contain modified amino acids, unusual linkages or altered chirality and may be regarded as fundamentally different from circular proteins produced by cyclization of a gene-coded precursor protein.

The circular peptides/proteins that are either known, or thought, to be of genetic origin include the cyclotides,[3] MCoTI-I/II[4,5] and SFTI-1[6,7] from plants, RTD-1/2/3[8,9] from rhesus monkeys, and several bacterial proteins, including microcin J25,[10−12] gassericin A,[13] bacteriocin AS-48,[14] and several pilin proteins.[15] The discovery and structures of such circular proteins have been recently reviewed.[1,16] Of the bacterial circular proteins microcin J25, referred to as MccJ25, is the smallest, with just 21 amino acids. It is secreted by certain strains of *Escherichia coli* to combat competing microbes under conditions of nutrient depletion. Its potent activity, with typical minimum inhibitory concentrations in the sub micromolar range, is mainly directed against *Enterobacteriaceae*, including several pathogenic strains of *Salmonella* and *Shigella*. Interestingly, recent studies have shown that MccJ25 appears to have a different mechanism of action against different species. In *E. coli* several resistant strains carrying mutations in conserved regions of RNA polymerase β' subunit have been isolated, indicating that MccJ25 acts by

(1) Trabi, M.; Craik, D. J. *Trends Biochem. Sci.* **2002**, *27*, 132−138.
(2) Kohli, R. M.; Walsh, C. T. *Chem. Commun. (Camb.)* **2003**, 297−307.
(3) Craik, D. J.; Daly, N. L.; Bond, T.; Waine, C. *J. Mol. Biol.* **1999**, *294*, 1327−1336.
(4) Heitz, A.; Hernandez, J. F.; Gagnon, J.; Hong, T. T.; Pham, T. T.; Nguyen, T. M.; Le-Nguyen, D.; Chiche, L. *Biochemistry* **2001**, *40*, 7973−7983.
(5) Hernandez, J. F.; Gagnon, J.; Chiche, L.; Nguyen, T. M.; Andrieu, J. P.; Heitz, A.; Trinh Hong, T.; Pham, T. T.; Le Nguyen, D. *Biochemistry* **2000**, *39*, 5722−5730.
(6) Korsinczky, M. L.; Schirra, H. J.; Rosengren, K. J.; West, J.; Condie, B. A.; Otvos, L.; Anderson, M. A.; Craik, D. J. *J. Mol. Biol.* **2001**, *311*, 579−591.
(7) Luckett, S.; Garcia, R. S.; Barker, J. J.; Konarev, A. V.; Shewry, P. R.; Clarke, A. R.; Brady, R. L. *J. Mol. Biol.* **1999**, *290*, 525−533.
(8) Tang, Y. Q.; Yuan, J.; Osapay, G.; Osapay, K.; Tran, D.; Miller, C. J.; Ouellette, A. J.; Selsted, M. E. *Science* **1999**, *286*, 498−502.
(9) Trabi, M.; Schirra, H. J.; Craik, D. J. *Biochemistry* **2001**, *40*, 4211−4221.
(10) Salomon, R. A.; Farias, R. N. *J. Bacteriol.* **1992**, *174*, 7428−7435.
(11) Blond, A.; Peduzzi, J.; Goulard, C.; Chiuchiolo, M. J.; Barthelemy, M.; Prigent, Y.; Salomon, R. A.; Farias, R. N.; Moreno, F.; Rebuffat, S. *Eur. J. Biochem.* **1999**, *259*, 747−755.
(12) Blond, A.; Cheminant, M.; Segalas-Milazzo, I.; Peduzzi, J.; Barthelemy, M.; Goulard, C.; Salomon, R.; Moreno, F.; Farias, R.; Rebuffat, S. *Eur. J. Biochem.* **2001**, *268*, 2124−2133.
(13) Kawai, Y.; Saito, T.; Kitazawa, H.; Itoh, T. *Biosci. Biotechnol. Biochem.* **1998**, *62*, 2438−2440.
(14) Gonzalez, C.; Langdon, G. M.; Bruix, M.; Galvez, A.; Valdivia, E.; Maqueda, M.; Rico, M. *Proc. Natl. Acad. Sci. U.S.A.* **2000**, *97*, 11221−11226.
(15) Kalkum, M.; Eisenbrandt, R.; Lurz, R.; Lanka, E. *Trends Microbiol.* **2002**, *10*, 382−387.
(16) Craik, D. J.; Daly, N. L.; Saska, I.; Trabi, M.; Rosengren, K. J. *J. Bacteriol.* **2003**, *185*, 4011−4021.

10.1021/ja0367703 CCC: $25.00

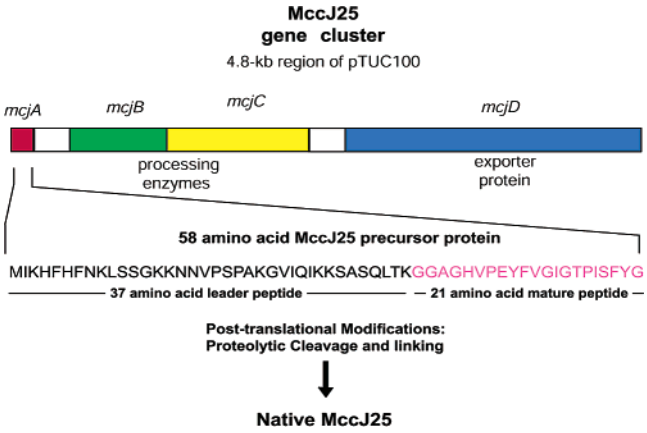

Figure 1. Sequence of the antimicrobial peptide microcin J25 and representation of its encoding genes. The 21 amino acid mature peptide (pink) is excised from a 58 amino acid precursor protein. Coded on the same plasmid as the microcin precursor *mcjA* are several other genes associated with maturation (*mcjB* and *mcjC*) and export (*mcjD*) of the mature peptide.

inhibiting gene translation.[17,18] In contrast, in *Salmonella newport*, MccJ25 has been shown to disrupt the cell membrane.[19]

The amino acid sequence (Figure 1) was first reported by Blond et al. in 1999[11] at about the same time as a plasmid-encoded gene corresponding to the amino acid sequence of a precursor protein was described.[20] The plasmid also contains several other genes that are implicated in processing of the precursor protein to facilitate maturation and export of MccJ25. On the basis of a range of amino acid sequencing, enzyme cleavage, mass spectrometry, and NMR data Blond et al.[11] surmised that mature MccJ25 was a head-to-tail cyclic peptide. They reported that the peptide had a compact three-dimensional structure as deduced by NMR data. It was proposed that the molecule contained a small region of β-strand secondary structure and that the circular backbone was folded back on itself in a well-defined structure. Blond et al.[12] commented on general similarities between this proposed structure and that of kalata B1, a prototypic member of the cyclotide family of circular plant proteins[3], characterized earlier in our laboratory.[21] This similarity is somewhat surprising given that the proposed primary structure for MccJ25 contains no cross-linking bonds to constrain the circular backbone. Indeed it is quite unusual for a small peptide to adopt such a well-defined structure in the absence of disulfide or other cross-linking bonds. In the case of the cyclotides, there is an especially constrained arrangement of their three disulfide bonds, referred to as a cystine knot[22,23] that stabilizes the fold and has been proposed to account for the remarkable thermal and chemical stability of the cyclotides as well as their resistance to enzymatic breakdown.[24] MccJ25 also appears to be extremely stable,[12] and it was intriguing to us that this stability could be achieved in such a small peptide without apparent cross-bracing.

Even more interesting was the recent report by Blond et al.,[25] which proposed that a thermolysin-cleaved analogue of MccJ25 maintained antimicrobial activity and a well-defined structure over most of the molecule, despite having a cleaved backbone. In particular, it was proposed that the β-strand region, which is distant from the enzyme cleavage site, was almost identical with the corresponding region in the native peptide. By contrast, a synthetic peptide of the same sequence as the thermolysin-cleaved peptide had neither biological activity nor a well-defined structure.[25] It was suggested that the folding of native MccJ25 might involve a "helper" molecule in vivo that assists in producing the compact three-dimensional structure.[25] Further, it was suggested that once formed, this structure is maintained in the enzyme-cleaved derivative but cannot be achieved by folding of synthetic peptide in vitro.[25]

Because of our interest in naturally occurring circular proteins and because of the unusual findings reported for the folding of MccJ25 we attempted to synthesize a linear derivative of this peptide, with the termini selected to correspond to the location of the natural termini coded by the gene sequence. For comparison, we also made a synthetic version of the putative head-to-tail cyclic peptide. However, as we report here, we found that neither product folded into well-defined three-dimensional structures nor behaved like the native peptide. Further investigation has led us to conclude that the original interpretation[12] of MccJ25 as a head-to-tail cyclized protein is incorrect. In fact, it incorporates a side chain-to-backbone cycle that protects the N-terminus and an unusual threaded structure that protects the C-terminus. We here report the three-dimensional structure of this fascinating natural product. Interest in the molecule arises because of its potent antibacterial activity and remarkable stability, so it is important to develop a structural basis for these properties.

Experimental Section

Synthesis of Linear MccJ25. Linear microcin J25 was assembled on Boc-Gly-OCH$_2$-PAM (Applied Biosystems, Foster City, CA) resin by manual solid-phase peptide synthesis using the in situ neutralization/HBTU protocol for Boc chemistry.[26] Amino acid side chain protection was as follows: Glu(OChx), His(DNP), Thr(Bzl) and Tyr(2-Br-Z). Prior to HF cleavage both the DNP and Nα-Boc groups were removed. Cleavage of the peptide from the resin was achieved using HF with *p*-cresol and *p*-thiocresol as scavengers (9:0.5:0.5 (v/v) HF:*p*-cresol:thiocresol). The reaction was allowed to proceed at −5 to 0 °C for 1 h; HF was removed under vacuum and the peptide precipitated with ether. Following cleavage, the peptide was dissolved in 50% acetonitrile containing 0.05% TFA and lyophilized. The crude peptide was purified by RP-HPLC on a Phenomenex C$_{18}$ column using a gradient of 0−80% B (Buffer A − H$_2$O/0.05% TFA, Buffer B − 90% MeCN/10% H$_2$O/0.045% TFA) in 80 min, and the eluent was monitored at 230 nm. These conditions were used in subsequent purification steps. Analytical RP-HPLC and ES−MS confirmed the purity and molecular mass of the synthesized peptide.

Synthesis of Head-to-Tail Cyclic MccJ25. The method used to synthesize head-to-tail cyclic MccJ25 was based on the procedure

(17) Delgado, M. A.; Rintoul, M. R.; Farias, R. N.; Salomon, R. A. *J. Bacteriol.* **2001**, *183*, 4543−4550.
(18) Yuzenkova, J.; Delgado, M.; Nechaev, S.; Savalia, D.; Epshtein, V.; Artsimovitch, I.; Mooney, R. A.; Landick, R.; Farias, R. N.; Salomon, R.; Severinov, K. *J. Biol. Chem.* **2002**, *277*, 50 867−50 875.
(19) Rintoul, M. R.; de Arcuri, B. F.; Salomon, R. A.; Farias, R. N.; Morero, R. D. *FEMS Microbiol. Lett.* **2001**, *204*, 265−270.
(20) Solbiati, J. O.; Ciaccio, M.; Farias, R. N.; Gonzalez-Pastor, J. E.; Moreno, F.; Salomon, R. A. *J. Bacteriol.* **1999**, *181*, 2659−2662.
(21) Saether, O.; Craik, D. J.; Campbell, I. D.; Sletten, K.; Juul, J.; Norman, D. G. *Biochemistry* **1995**, *34*, 4147−4158.
(22) Craik, D. J.; Daly, N. L.; Waine, C. *Toxicon* **2001**, *39*, 43−60.
(23) Pallaghy, P. K.; Nielsen, K. J.; Craik, D. J.; Norton, R. S. *Protein Sci.* **1994**, *3*, 1833−1839.
(24) Craik, D. J.; Simonsen, S.; Daly, N. L. *Curr. Opin. Drug Discov. Devel.* **2002**, *5*, 251−260.
(25) Blond, A.; Cheminant, M.; Destoumieux-Garzon, D.; Segalas-Milazzo, I.; Peduzzi, J.; Goulard, C.; Rebuffat, S. *Eur. J. Biochem.* **2002**, *269*, 6212−6222.
(26) Schnölzer, M.; Alewood, P.; Jones, A.; Alewood, D.; Kent, S. B. H. *Int. J. Pept. Protein Res.* **1992**, *40*, 180−193.

described by Yan and Dawson.[27] *S*-Trityl β-mercaptopropionic acid (0.75 mmol) in DMF was activated with 0.75 mmol of HBTU and 1.5 mmol of DIEA and coupled to 0.5 mmol Leu-OCH_2−PAM resin (2 × 20 min, 99.9% yield). The trityl-protecting group was then removed by 2 × 1 min treatments with 2.5% triisopropylsilane and 2.5% H_2O in TFA. These reactions formed the TAMPAL linker, which results in a C-terminal thioester on cleavage of the peptide from the resin. The peptide chain (CGHVPEYFVGIGTPISFYGGG) was then constructed using standard Boc in situ neutralization chemistry. The residue corresponding to Ala3 in MccJ25 was replaced with a Cys to facilitate the native chemical ligation reaction. The DNP protecting group was not removed prior to cleavage, as the conditions required for deprotection are not compatible with the TAMPAL/thioester linker. The peptide chain with the C-terminal thioester was cleaved from the resin using HF with *p*-cresol as a scavenger (9:1 (v/v) HF:*p*-cresol). The crude peptide was then purified by RP-HPLC as described above.

The linear peptide was cyclized by incubating it in 0.1M NH_4HCO_3 (pH 8.5) overnight at room temperature. The DNP protecting group was then removed from the His by addition of 10 equiv of MESNA to the cyclization buffer with incubation at room temperature for 1 h. The mixture was then purified by RP-HPLC to yield the cyclic peptide. Desulfurization of the cysteine to produce Ala3 was achieved by incubating it in 20% AcOH with Raney Nickel for 2 hours.[27] The reaction mixture was filtered, diluted with buffer A and purified by RP-HPLC.

Cyclization of Linear MccJ25. 100 μg of linear MccJ25 (0.05 μmol) was dissolved in 1 mL of dimethylformamide (DMF). A 100× molar excess of DIEA was added followed by a 10× molar excess of HBTU (0.005 M solution in DMF). The reaction mixture was left for five minutes at room temperature then diluted with buffer A. The reaction products were analyzed by RP-HPLC and ES−MS.

Methylation of Native MccJ25. For methylation of MccJ25 methanolic HCl was prepared by adding 400 μL acetyl chloride to 2.5 mL methanol.[28] 30 μL of this reagent was then added to approximately 0.5 μg of native MccJ25, which then was incubated at room temperature for 2 h. The reaction was terminated by injection on narrowbore RP-HPLC (Agilent Poroshell 2.1 × 75 mm), and the methylated product was manually collected and dried in a speedvac. The sample was reconstituted in 10 μL 60% methanol in water containing 0.1% formic acid before analysis on the QSTAR Pulsar system as described below.

Mass Spectrometry. Full scan, *m*/*z* 400−2000, molecular weight determination was performed on a QSTAR Pulsar, hybrid quadrupole, QqTOF mass spectrometer (Applied Biosystems, California, USA), equipped with a nanoelectrospray ion source (Protana, Odense, Denmark). An aliquot (1 μL) of the NMR sample was dissolved in 50/50 MeCN/0.1% formic acid and was analyzed in the positive-ion detection mode with a potential of 900 V applied to the nanospray needle.

Tandem mass spectrometric, MS/MS product ion analysis was performed on the same aliquot and positive-ion potential as above and with a collision energy of between 15 and 55 eV. BioAnalyst 1.1 software (Applied Biosystems, California, USA) was used to aid data interpretation.

For MS^n a nanospray-ion trap MS (Protana's NanoES source (MDS Protana A/S, Odense, Denmark) mounted on a LCQ (Thermo Finnigan, San Jose, USA)) was used. Native MccJ25 was analyzed in the positive ion mode at a concentration of ca. 0.1 μg/μL in 60% MeOH with 1% HOAc. The spray voltage was set at 4 kV and the capillary temperature at 200 °C. Ions were isolated with a width of 3 amu, except for the final stage of MS when a width of 2 amu was used. The CID was set individually for the different experiments; typical values ranged between 40 and 55%.

NMR Spectroscopy. Samples for NMR spectroscopy contained 5 mg of synthetic linear MccJ25 or 2 mg of synthetic macrocyclic MccJ25 dissolved in 0.5 mL of 100% (D_3)MeOH, 50% (D_3)MeOH/50% H_2O or 50% (D_3)MeOH/50% (D_3)MeCN. The sample of native MccJ25 contained ∼0.2 mg of MccJ25 dissolved in 0.125 mL of (D_3)MeOH. Some additional spectra were recorded in which 10−40% H_2O was titrated into the (D_3)MeOH solution. For the synthetic material all spectral data, including TOCSY[29] and NOESY[30] spectra were recorded at 750 MHz on a Bruker DMX spectrometer equipped with triple resonance probe while for native MccJ25 spectral data were acquired both at 750 MHz using a triple resonance microprobe and at 500 MHz using a Bruker Avance spectrometer equipped with a cryogenic probe. The carrier frequency was in all experiments set at the center of the spectrum, on the water resonance frequency. All spectra were acquired in phase sensitive mode using TPPI.[31] The following homonuclear spectra were recorded: TOCSY with an MLEV17[32] isotropic mixing period of 80ms, ECOSY,[33] and NOESY with mixing times of 100 ms and 250 ms. For the ECOSY experiment, the solvent proton signal was suppressed by low power irradiation during the relaxation delay (1.8 s). Solvent suppression in TOCSY and NOESY experiments was achieved using a modified WATERGATE[34] sequence in which two gradient pulses of 1ms duration and 6 G cm^{-1} strength were applied on either side of the binomial pulse. 2D spectra were generally collected over 4096 data points in the f2-dimension and 512 increments in the f1-dimension over a spectral width corresponding to 11 ppm.

All spectra were processed on a Silicon Graphics workstation using XwinNMR (Bruker). The f1-dimension was generally zero-filled to 1024 real data points with the f1 and f2-dimensions being multiplied by a sine-squared function shifted by 90° prior to Fourier transformation. Spectra were referenced to the solvent resonance. Spectra were analyzed within the program XEASY,[35] and assignments of NOE cross-peaks were performed both manually and automatically by the automatic assignment program CANDID,[36] which is a part of the CYANA package.

Structure Calculations. Cross-peaks in NOESY spectra recorded at 295 K at 500 and 750 MHz with a mixing time of 250 ms were integrated and calibrated and distance constraints were derived using CYANA. Backbone dihedral angles restraints were derived from $^3J_{HN\alpha}$ coupling constants measured from amide signal splitting in the 1D spectrum. Angles were restrained to $-120° \pm 30°$ for $^3J_{HN\alpha} > 9$ Hz (Ala3, Val6, Glu8, Thr15, Ile17, and Phe19). Additional ϕ angle restraints were applied where the intraresidue dαN(i,i) NOE was clearly weaker than the sequential dαN(i,i+1) NOE. In all cases, measured coupling constants were in agreement with those reported by Blond et al.[12]

Stereospecific assignments of β-methylene protons and $\chi1$ dihedral angles were derived from $^3J_{\alpha\beta}$ coupling constants, measured from ECOSY spectra, in combination with NOE peak intensities. The $\chi1$ angles were restrained to $60° \pm 30°$ (Ser18) or $-60° \pm 30°$ (His5, Glu8, Tyr9, and Phe10) based on the observed coupling constants and NOE patterns, as specified by Wagner.[37] Stereospecific assignments for Pro residues were due to the fixed geometry based on NOE intensities of the intra residual cross-peaks.

Structures were analyzed for the presence of hydrogen bonds. No deuterium exchange data were recorded due to a limited amount of

(27) Yan, L. Z.; Dawson, P. E. *J. Am. Chem. Soc.* **2001**, *123*, 526−533.
(28) Hunt, D. F.; Yates, J. R., 3rd; Shabanowitz, J.; Winston, S.; Hauer, C. R. *Proc. Natl. Acad. Sci. U.S.A.* **1986**, *83*, 6233−6237.
(29) Braunschweiler, L.; Ernst, R. R. *J. Magn. Reson.* **1983**, *53*, 521−528.
(30) Jeener, J.; Meier, B. H.; Bachmann, P.; Ernst, R. R. *J. Chem. Phys.* **1979**, *71*, 4546−4553.
(31) Marion, D.; Wüthrich, K. *Biochem. Biophys. Res. Commun.* **1983**, *113*, 967−974.
(32) Bax, A.; Davis, D. G. *J. Magn. Reson.* **1985**, *65*, 355−360.
(33) Griesinger, C.; Sørensen, O. W.; Ernst, R. R. *J. Magn. Reson.* **1987**, *75*, 474−492.
(34) Piotto, M.; Saudek, V.; Sklenar, V. *J. Biomol. NMR* **1992**, *2*, 661−665.
(35) Eccles, C.; Guntert, P.; Billeter, M.; Wüthrich, K. *J. Biomol. NMR* **1991**, *1*, 111−130.
(36) Herrmann, T.; Guntert, P.; Wuthrich, K. *J. Mol. Biol.* **2002**, *319*, 209−227.
(37) Wagner, G. *Prog. NMR Spectrosc.* **1990**, *22*, 101−139.

native MccJ25. However, Blond et al.[12] reported that several amide protons showed slow exchange with the solvent, including Glu8, Phe19, and Tyr20, for which the amide signals were still visible after 2 days. These protons were deduced, after initial structure calculations, to be associated with the carbonyl oxygens of Ser18, Gly2, and Val6 respectively, and restraints for these hydrogen bonds were included in the final round of structure calculations. Further, most other amide protons with slow or medium exchange rates appear to be involved in hydrogen bonds in the calculated structure, indicating that it represents a good model of MccJ25.

Structures were calculated using simulated annealing and energy minimization protocols within XPLOR[38] and CNS.[39] To evaluate whether using our standard protocols, which include structure refinement in explicit water, would provide a good model of the structure even though the spectral data were recorded in methanol, we calculated structures in a vacuum in parallel but concluded that the choice of solvent in the refinement process had little or no effect on the final structures. The final set of structures was generated in CNS using protocols from the program ARIA.[40] These protocols involve torsion angle simulated annealing dynamics and refinement by Cartesian dynamics in the presence of solvent. The coordinates for this structural family have been submitted to the PDB and given the accession code 1Q71.

Results

The original rationale for undertaking this study was to compare a linear derivative of MccJ25 with the presumed cyclic peptide in order to gain an insight into the factors contributing to the apparently well defined three-dimensional structure of native MccJ25. A linear version of MccJ25 corresponding to the gene sequence (Figure 1) was synthesized using solid phase peptide chemistry and, after purification using HPLC, yielded a peptide with exactly the expected mass (2124 Da), as judged by ES-TOF MS. This is 18 mass units heavier than the reported value (2106 Da) for the native peptide, consistent with the latter having undergone a single cyclization or dehydration event.

The synthetic linear peptide was soluble at millimolar concentrations in methanol, as is the case for the native peptide. Two-dimensional NMR spectra were recorded and indicated that although a small fraction of the peptide appeared to be folded, multiple conformations were present (judging by the number and intensity of peaks) and the main signals corresponded to a form that appeared not to have a well-defined three-dimensional structure. This deduction was made based on the poor dispersion of signals in the amide region of the spectrum, the lack of any upfield shifted methyl signals and the general broadness of the spectral lines for a peptide of this size. Further, although the spectra in methanol solution were monitored over ~2 days, peaks from the minor, apparently folded, conformations disappeared and the remaining signals were indicative of a conformation that was clearly unfolded. The αH NMR chemical shifts of this conformer were determined (data not shown) and were close to random coil values, supporting this conclusion.

A cyclic version of the peptide was then prepared using the procedure described by Yan and Dawson[27] in which native chemical ligation is first used to achieve head-to-tail cyclization and then an introduced Cys residue necessary for chemical reactivity of the C-terminus with the N-terminus is desulfurized to convert it to Ala. As with the linear derivative, this peptide was purified by RP-HPLC and yielded a peptide with a mass (2106 Da) in agreement with the theoretical value. However, as was the case for the linear peptide, the cyclic molecule also appeared to be devoid of a well-defined three-dimensional structure as assessed by ^{1}H NMR spectroscopy. Overlap of the NMR signals was so severe that it was not possible to fully assign them to individual protons.

We attempted to refold the synthetic head-to-tail cyclic peptide using a range of conditions, including water/methanol and water/acetonitrile mixtures, but were unable to achieve a product that had spectral characteristics similar to those reported for the native peptide. At this point, it became of interest to reexamine the evidence that the native peptide was in fact cyclic.

The reported three-dimensional structure of MccJ25[12] comprises a very compact fold with a large number of close inter-proton contacts. For such a fold, one would expect to observe a large number of medium and long range NOEs between residues in the protein core. However, only a rather small number of such NOEs (<25) were used in the published structure calculations. In fact, when analyzing the fold in more detail it becomes apparent that the structure does not fully agree with the experimental data. This is particularly evident from the presence of more than 25 inter-proton distances consistently closer than 3.5 Å for which no corresponding NOEs are visible in the spectra or reported in the published restraints list, and whose absence cannot be explained by signal overlap. Further, and more significantly, there are no sequential NOEs linking the two Gly residues that form the N- and C-terminal residues deduced from the gene sequence. Such NOEs would be expected for a backbone cyclized peptide. Sequential $H\alpha_i-HN_{i+1}$ NOEs are observed throughout the entire sequence of MccJ25 except for across the proposed peptide bond between Gly1 and Gly21, strongly suggesting that the termini are in fact not covalently linked.

In NMR spectra of linear peptides no amide signal is generally observed for the N-terminal residue due to the fast solvent exchange of protons in free amines. However, in MccJ25 the amide signal of Gly1 is clearly visible, indicating that the N-terminus is indeed modified in some way. To find an explanation for this other than in terms of a cyclic backbone we explored the possibility of side chain-to-backbone linkages. The NMR spectra revealed the presence of several NOEs between the amide proton of Gly1 and the side chain protons of Glu8. On the basis of this observation we hypothesized that the cyclization event might involve Gly1 and Glu8 rather than Gly1 and the C-terminus. This would result in the structure containing an eight-residue ring in the N-terminal half of the molecule with a linear tail for the C-terminus, so that the molecule would resemble a lasso.

Mass Spectrometry. To characterize MccJ25 in more detail and to gain definitive evidence to distinguish between a circular backbone or an N-terminal ring we subjected both native MccJ25 and the macrocyclic material generated by chemical synthesis to extensive analysis by mass spectrometry. For both peptides an identical monoisotopic mass of 2106.0 Da was determined from the mass of 1054.0 observed for the $(M+2H)^{2+}$ ion. This corresponds well with the theoretical mass of 2106.02 for the 21 amino acids in the primary sequence minus 18 Da consistent with a single dehydration as observed in cyclic peptides. However, the mass profiles observed for the two

(38) Brünger, A. T. *X-PLOR Manual Version 3.851*; Yale University: New Haven, CT, 1996.
(39) Brünger, A. T.; Adams, P. D.; Rice, L. M. *Structure* **1997**, *5*, 325−336.
(40) Linge, J. P.; Nilges, M. *J. Biomol. NMR* **1999**, *13*, 51−59.

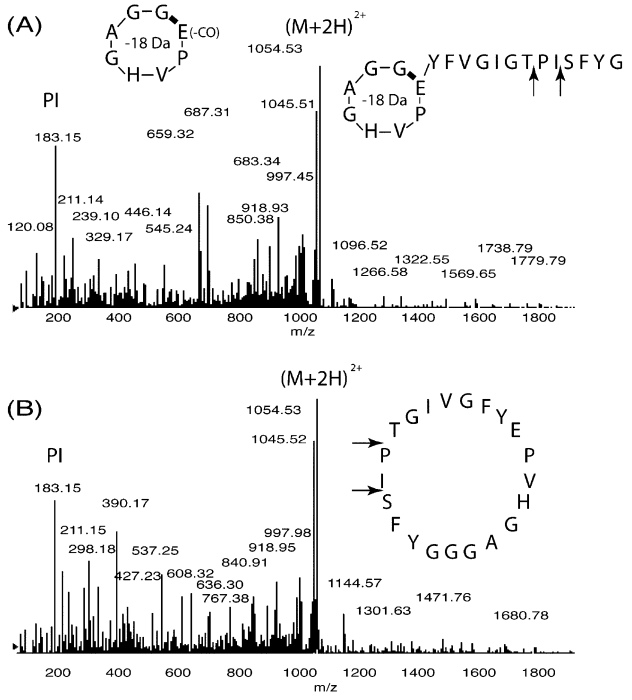

Figure 2. MS fragmentation of native and synthetic MccJ25, with (A) and (B) showing their respective MS/MS spectra. The parent ions (*m*/*z* 1054) are labeled with $(M+2H)^{2+}$. The fragmentation patterns are clearly different between the two forms of MccJ25. For the native form the peaks *m*/*z* 687.3/659.3, which are absent in the synthetic material, dominate in the low mass region. These peaks correspond to an N-terminal ring structure formed by a linkage between Gly1 and the side chain of Glu8, as illustrated by the thickened bond in the inset structures. The primary sequences are inset on the spectra and highlight the internal linkage and macrocyclic structures of the native and synthetic forms, respectively. The major cleavage sites for fragmentation are indicated on these insets with arrows. Some fragments are present in both forms, including the peaks that correspond to the internal fragment PI (*m*/*z* 211.1/183.1). The spectra were obtained using QSTAR MS.

peptides differ in that although the native material has a preference for absorbing two charges the main species of the synthetic material carries three charges, suggesting a less compact structure. When subjected to MS/MS both peptides show, as expected for cyclic or cross-linked peptides, a rather complicated composition of masses due to internal fragmentation. Although the spectra are similar in that the main break points for both peptides are around the Pro residues the fragment profiles observed are clearly different (Figure 2). After careful analysis, we concluded that all major fragments can be assigned to standard ions corresponding to a handful of fragmentation series as outlined in Figure 3. A table with the masses of the derived fragments is provided as supplementary information.

For native MccJ25 there were basically three types of fragments observed. First, there were fragments corresponding to the C-terminal region that were consistent with there being a free C-terminus. This y-series (Figure 3A, series I) was followed from HO-Gly21-Tyr20 (the y_2-ion, *m*/*z* 239.1) to HO-Gly21-Tyr9 (y_{13}, *m*/*z* 1419.7). Internal shorter fragments originating from this sequence were also detected as shown in Figure 2A, series II. The presence of a free C-terminus is clearly inconsistent with the head-to-tail macrocyclic model.

The second family of fragments was N-terminal to a major cleavage site adjacent to Pro16. The b- and a-series (referring to amide bond cleavage and the additional loss of the carbonyl group of these fragments, respectively) were easily followed from Thr15 (b_{15}/a_{15}, *m*/*z* 1424.7/1396.7) to Glu8 (b_8/a_8 ions, *m*/*z* 687.3/659.3) as shown in Figure 3A, Series III. However, all these fragments showed a mass 18 Da less than expected, consistent with a cyclization/dehydration in the N-terminal part of the peptide. Dominant in this series are the b_8/a_8 ions, which according to the new structure proposed here are consistent with the ring formed by side chain cyclization of Glu8 to the N-terminal of Gly1. A large number of fragments are seen below the b_8/a_8 ion pair that may be attributed to internal fragmentation (Figure 3A, series IV). To unambiguously confirm the identity of these ions and to examine if their fragmentation patterns could give any more information regarding the ring structure, we subjected these ions to MS^n experiments using nanospray ion trap MS.

MS^3 of the b_8 ion (*m*/*z* 687) gave 659 and 588 as major fragments corresponding to the respective loss of the C-terminal carbonyl of Glu8 (−28), and ring opening C-terminally of Val6 with the subsequent loss of this residue (−99) as shown in Figure 3A, Series IV. MS^4 of the 588 fragment confirmed this ring opening and in combination with the MS^3 data the sequence VHGA(323) could be determined. The remaining mass equals the mass calculated for GGEP, with the loss of water due to cyclization included.

Fragmentation by MS^3 of the a_8 ion (*m*/*z* 659) gave 545 and 446 as major fragments. The 545 ion, corresponding to a loss of −114 fitted nicely with the loss of Gly1-Gly2. However, no further ions supporting this fragmentation could be found. Together with MS^4 experiments on the two main fragments all data indicated that the cleavage instead occurred between the α-carbon and the NH group of the Glu8 residue in combination with a hitherto not characterized rearrangement. Taking this into account the following sequence could be confirmed (180)-AGHVP(17), where 180 corresponds to GGE(−17) including the loss of water and the Glu8 C-terminal carbonyl group.

In summary, the MS^n experiments confirmed two fragmentation series, originating from two different cleavage sites that overlapped each other. Both of these series also overlapped the Gly1-Glu8 linkage, and thus confirmed the presence of the ring.

The third type of fragments contained both N-terminal and C-terminal parts of the molecule. These are represented in Figure 3A, series V and VI. Steric hindrance between the ring and the bulky side chains of a putatively threaded C-terminal part of the peptide most likely explains this remarkable fragmentation pattern.

To confirm the presence of a free C-terminal MS/MS was also done on methylated MccJ25. This experiment showed an increase of 14 amu of all fragmentation series containing the C-terminal part of the peptide. Of these, the series y_2 (methylated YG, *m*/*z* 253.1) to y_6 (*m*/*z* 697.4) was easily followed. This particular series establishes the C-terminal part (i.e., YG) as the site of methylation, however it does not exclude the possibility of Tyr20 as the methylation site (even if this seems highly unlikely). As for the native sample, some internal fragmentation series dominated in the low mass region of the spectra, and of these the series Pro16-Ile17 to Pro16-Gly21 proved valuable in unambiguously determining Gly21 as the site of methylation: the masses of this series are in absolute agreement with the native peptide sequence up to the b- and a-ions of Pro16-Tyr20 (*m*/*z* 608.3/580.3) thus excluding Tyr20 as the methylated residue. N-terminal fragments of the methy-

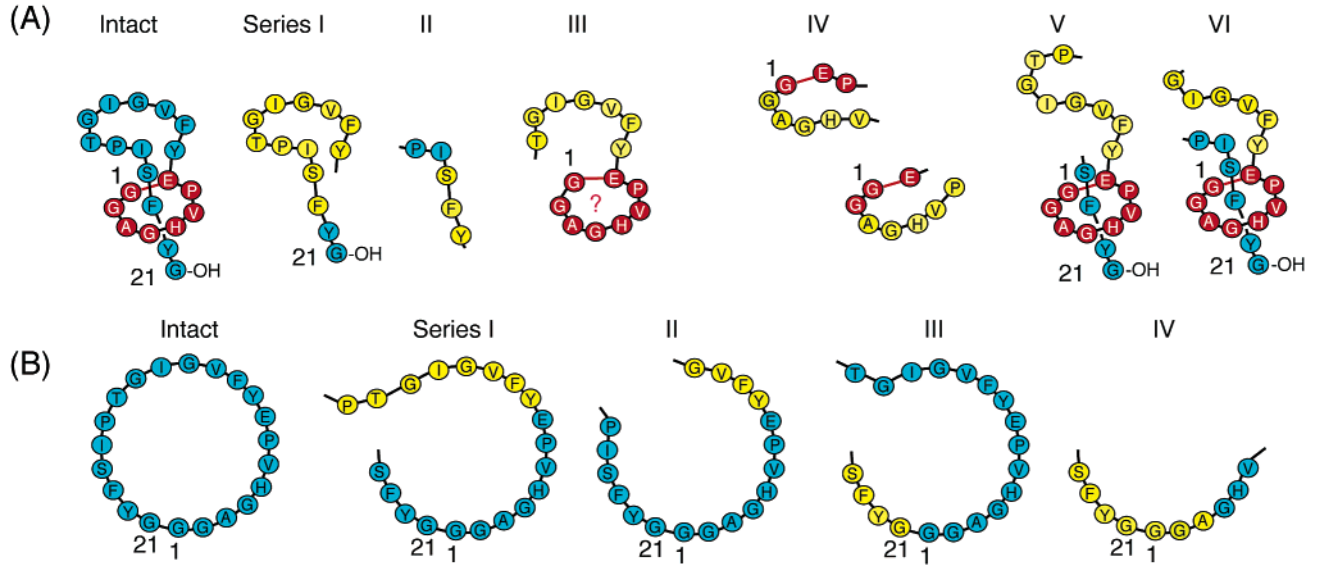

Figure 3. Schematic representation of the fragments derived from the MS/MS analysis. (A) and (B) represent starting points for fragmentation series observed for native and synthetic cyclic MccJ25, respectively. All residues are represented by their single letter amino acid codes with Gly1 and Gly21 numbered. Yellow colored amino acids reflect fragment series where ions corresponding to the removal of each successive amino acid are observed. Blue and red colors represent amino acids corresponding to the C-terminus and the N-terminal ring, respectively. In summary the fragmentation patterns show a free hydroxylated (or after methylation, methylated) C-terminal (A, Series I), some dominant internal fragments (A, Series II), a cyclized/dehydrated N-terminal part of the peptide (A, Series III) and confirmed the Gly1-Glu8 ring structure of the native material (A, Series IV). Moreover, the ring structure is so tightly associated with the C-terminal tail that although the peptide chain is broken the two fragments exist as one entity under MS/MS conditions (A, Series V, VI). Although these MS data do not define the nature of the noncovalent association, NMR studies suggest that it is due to threading of the C-terminal tail through the embedded ring. The macrocyclic synthetic form shows none of these characteristics seen for the native MccJ25, but its fragmentation is consistent with a true macrocyclic structure (B, Series I−IV).

lated peptide showed molecular weights identical to those of native MccJ25, confirming that no modification(s) had occurred in this part of the peptide. This included the dominant peaks identified as the b_8/a_8 ions and their respective internal fragmentations as assigned in the MS^n experiments for the native peptide, as well as the continuing stretch of these ions up to b_{13}/a_{13}. The absence of methylation of Glu8 is congruent with its involvement in a side-chain linkage.

For the macrocyclic synthetic material several series of fragments were identified, yielding almost complete sequence coverage, including a series overlapping the synthetically joined N- and C-termini as shown in Figure 3B. This clearly showed the true macrocyclic nature of this synthetic peptide, with a primary sequence identical to the one described for MccJ25 in the literature. As expected for a macrocyclic structure, the observed series of fragments originated from several sites of backbone cleavage. None of the fragmentation characteristics for this synthetic peptide were observed for the native one.

NMR Structure Determination. To further examine whether the NMR data supported a link between Gly1 and Glu8 we calculated a set of structures incorporating this side chain linkage in place of the N−C backbone linkage using the published distance and angular restraints.[12] The results showed that it was indeed possible to generate such structures without major violations of the experimental data. More interestingly, the structures adopted a fold in which the C-terminus is threaded through the ring structure formed by the Gly1-Glu8 linkage. We then undertook further refinement of the structure by cross validating and incorporating additional NOEs derived from NMR spectra recorded in our laboratory at 750 MHz. The final set of restraints comprised 112 inter-residual distance restraints, including 50 medium- and long-range distances and 12 backbone and 5 side chain dihedral angle restraints. Finally, six restraints

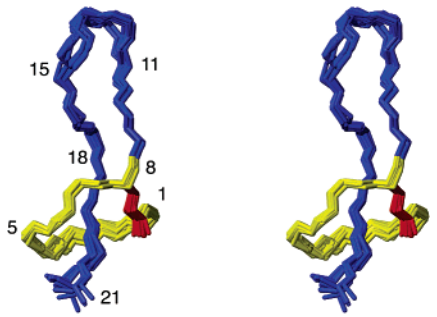

Figure 4. Twenty lowest energy structures selected to represent the solution structure of MccJ25 shown in stereoview. The structures are superimposed over all backbone atoms. Residues 1−8 (shown in yellow) together with the link between the N-terminus and Glu8 side chain (red) form a ring through which the C-terminal is threaded.

for three hydrogen bonds were included based on consistent close proximity between the partners in the preliminary structures and very slow solvent exchange rates reported by Blond et al.[12] From the final round of calculations, a family of 20 structures was chosen to represent the solution structure of MccJ25 based on low energies and minimal violations of the experimental data. The structures all have good covalent geometry and no distance or angular violations exceeding 0.2 Å or 2°, respectively. An analysis of close inter-proton contacts shows that the revised structures are significantly more consistent with the NOE data than the original structure. Only two distances not supported by the NOE data are consistently closer than 3.5 Å, but this is readily explained by the low sample concentration used.

Figure 4 shows a stereoview of the structural family superimposed over the backbone atoms and the structural and energetic statistics are summarized in Table 1. From this, it is clear that the structure is generally well defined with the

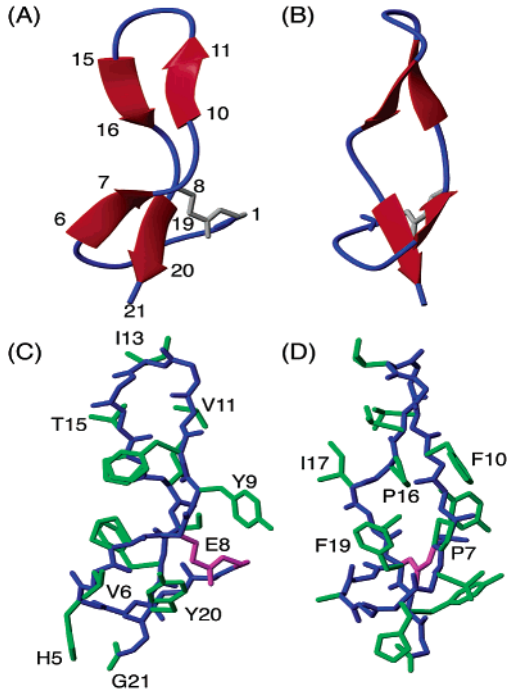

Figure 5. Ribbon representation of the lowest energy structure of MccJ25 illustrating the main elements of secondary structure; two small antiparallel β-sheets (A and B). In panels C and D the backbone is shown in blue, side chain heavy atoms in green and the Gly1-Glu8 link in magenta. The structure reveals the presence of two hydrophobic patches (Val6-Tyr20-Glu8 and Phe19-Pro7-Phe10-Pro16) as well as an electrostatic interaction between the C-terminus and His5. Selected residues are labeled with residue numbers and single letter amino acid codes. Views (B) and (D) are rotated 90° in relation to (A) and (C).

Table 1: Structural and Energetic Statistics for the Family of 20 Structures Selected to Represent the Solution Structure of MccJ25

energies:	(kcal/mol)
overall	-646 ± 28
bond	3.1 ± 0.3
angle	20 ± 2.3
van der Waals	-51 ± 7.2
NOE	4.8 ± 1.1
cdih	0.10 ± 0.08
dihed	78 ± 4.8
elec	-703 ± 28
RMSD:	
bond (Å)	0.0032 ± 0.0002
angle (°)	0.49 ± 0.03
improper (Å)	0.34 ± 0.04
residues 1−21 and backbone atoms (Å)	0.72 ± 0.22
and heavy atoms (Å)	1.26 ± 0.23
Ramachandran:	
most favored	53%
additionally allowed	46%
generously allowed	1%

exception of the turn involving residues 11−14. This may result from a lack of experimental restraints, however the absence of medium and long-range NOEs in this area together with chemical shifts close to random coil suggests that there may be some flexibility in this region.

Description of the Three-Dimensional Structure. The structure of MccJ25 can be described as a noose in which residues 1−8, together with the Gly1-Glu8 link, forms a loop through which the C-terminus threads. As shown in Figure 5, the fold is characterized by two small antiparallel β-sheets, each comprising two strands. The first sheet comprises residues 6−7 and 18−19 and is formed between part of the ring and the penetrating C-terminal segment. The second sheet, which involves residues 10−11 and 15−16, is associated with a β-turn involving residues 11−14, and forms a hairpin like structure. Although there is some ambiguity in the geometry of the turn, in most structures it can be classified as a type I β-turn.

The main interactions stabilizing the fold are van der Waals interactions between the amino acid side chains, which are predominantly hydrophobic in nature, and between polar groups in the backbone. Two main hydrophobic patches are present on the surface, with the first patch involving Tyr20, Val6, and the methylene groups of the Glu8 side chain and the second patch formed by the side chains of Pro7, Phe10, Pro16, and Phe19. With the N-terminus and Glu8 linked by an additional amide bond, MccJ25 carries only two charges, His5 and the C-terminus. Interestingly the structure reveals that these charges are very close, suggesting an electrostatic interaction, possibly in the form of a salt bridge. Such an interaction might play a major role in stabilizing the threaded structure. Furthermore, the structure reveals the presence of a number of hydrogen bonds in the hairpin as well as between the ring and the penetrating C-terminal backbone segment. To confirm the proposed noose-like structure we attempted to synthesize a derivative containing the side chain-to-backbone linkage. This was done via a nonspecific coupling reaction that also yielded some of the head-to-tail cyclized peptide (Figure 6). The Gly1 to Gly21 cyclic product and the Gly1 to Glu8 cyclic products had identical masses and different retention times, as expected, but neither corresponded exactly with the native peptide. We believe that this reflects the fact that while the Gly1 to Glu8 cyclic product has the correct primary structure, it probably lacks the noose threading of the native material. This is supported by MS/MS fragmentation of this peptide, which shows similar fragmentation series to native MccJ25 but lacks the characteristic fragments caused by the threading of the C-terminal through the ring. For example, the C-terminal y-fragments can be followed from y_2 to y_{13}, corresponding to Series I in Figure 3A, and the N-terminal b-fragments from b_8 to b_{19}, corresponding to Series III in Figure 3A. However, no ions corresponding to the threaded structure, as seen for native MccJ25 (Figure 3A series V and VI), can be observed.

Discussion

In the current study, we have shown that the potent antibacterial peptide MccJ25 does not have a head-to-tail cyclized backbone as originally reported[11] but instead incorporates an unusual backbone-to-side chain linkage that is penetrated by the C-terminal tail in a noose-like motif. It is these features that are responsible for the well-defined three-dimensional fold of the peptide. The secondary structure of MccJ25 is characterized by two small antiparallel β-sheets each comprising two strands. The revised structure is consistent with previously reported enzyme cleavage studies on the peptide and with its high stability and biophysical properties.[25] Due to the poor solubility of MccJ25 in water the structure was determined in methanol, however the threaded arrangement and compact fold suggests that the structure will not be significantly affected by solvent. This was supported by NMR spectra that showed no significant change in αH chemical shifts on titration of 40% H_2O into the methanol solution.

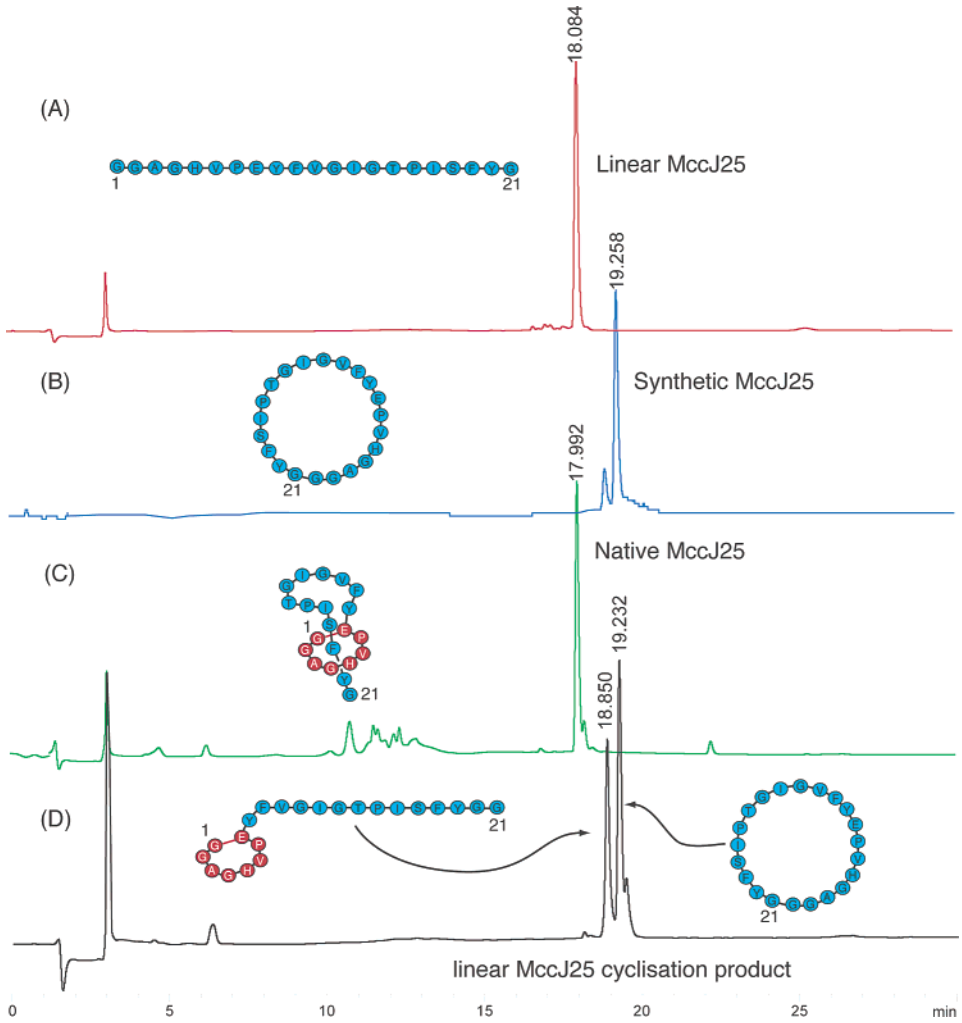

Figure 6. HPLC traces of linear (A), macrocyclic (B), native (C) MccJ25. As shown in panel (D) two products are produced when linear MccJ25 is treated with DMF/DIEA and HBTU. One product corresponds to the macrocylic material and the other contains a N-terminus to Glu8 linker. However, the latter does not have the same retention time as native most likely because the C-terminus is not threaded through the Gly1-Glu8 ring.

MS/MS analysis was not performed in the original studies aimed at elucidating the sequence of MccJ25 and the available NMR data were broadly consistent with the presence of an N-to-C cyclized backbone.[11] However, in the current study MS data and a new NMR analysis has provided additional information that has enabled the revision of the primary structure of MccJ25. The fragments in the MS analysis clearly show the presence of a free C-terminus and a linkage between residues Gly1 to Glu8. An attempt to make a synthetic derivative of MccJ25 containing this linkage yielded a compound having the proposed primary structure, but a different retention time on RP-HPLC to the native peptide, suggesting an alternative conformation. Including the backbone-to-side chain linkage in NMR-derived structure calculations for MccJ25 revealed that the ring formed by residues 1 to 8 is penetrated by residues 18 to 21. On the basis of the synthetic chemistry data this tightly constrained structure is apparently not accessible after formation of the linkage. Presumably the in vivo biosynthetic pathway facilitates correct folding before the "noose" is formed.

As a part of the MS analyses native MccJ25 was subjected to methylation. This modification adds +14 amu at acidic groups of a protein, that is to the side chains of Glu and Asp and to the C-terminal carboxyl group. The MS of methylated MccJ25 showed a Mw of 2120.0 corresponding to only one modification site. This result is consistent with both the structure proposed here, which contains a free C-terminal, and with the previous macrocyclic structure that contains a free Glu side chain. However, analysis by MS/MS of the methylated sample unambiguously showed that the modification site was indeed Gly21, congruent with the free C-terminal of the structure presented in the current study. For the N-terminal part of the peptide, the methylated sample showed the same dehydrated fragmentation series as for nonmodified native microcin. This included the dominant ions and series assigned through MS/MS and MS^n experiments as directly corresponding to the Gly1-Glu8 ring formation. In addition, none of these characteristic fragmentation patterns could be observed for the synthetic macrocyclic analogue. Together the MS data provided conclusive evidence for the structure presented in the current study, and unambiguously excluded the possibility of a head-to-tail macrocyclic peptide backbone as suggested previously.

The revised structure of MccJ25 provides an explanation for its behavior upon enzyme cleavage and during mass spectrometry analysis. For instance, Blond et al.[25] found that MccJ25 could not be digested by endoprotease GluC (V8 protease), despite Glu8 being relatively exposed in the three-dimensional macrocyclic structure. In our revised structure Glu8 is involved in a cross-link and thus would not be expected to be targeted

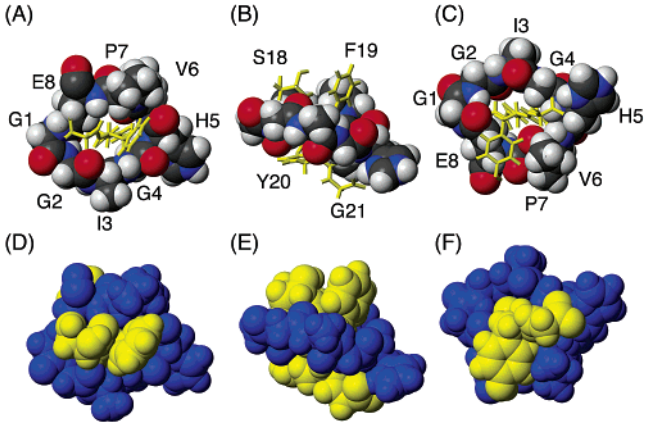

Figure 7. Interactions between the C-terminus (residues 18−21) of MccJ25 and the Gly1-Glu8 ring. Views (A), (B), and (C) show residues 18−21 in stick and the ring in space-filling representation with atoms color coded white, gray, red and blue corresponding to hydrogens, carbons, oxygens and nitrogens, respectively. The ring is penetrated by the C-terminal leaving Ser18 and Phe19 on one side of the ring and Tyr20 and Gly 21 on the other. As evident from views (D), (E), and (F), which show both the ring and the C-terminal in space-filling representation, the bulky side chains of Phe19 and Tyr20 prevent the peptide chain from slipping through the ring and thus account for the remarkable stability of both the native and thermolysin linearized peptides. All atoms are shown with a diameter corresponding to their van der Waals radii. Residues are labeled with numbers and single letter amino acid codes. Views (B, E) and (C, F) are rotated 90° and 180° respectively in relation to (A, D).

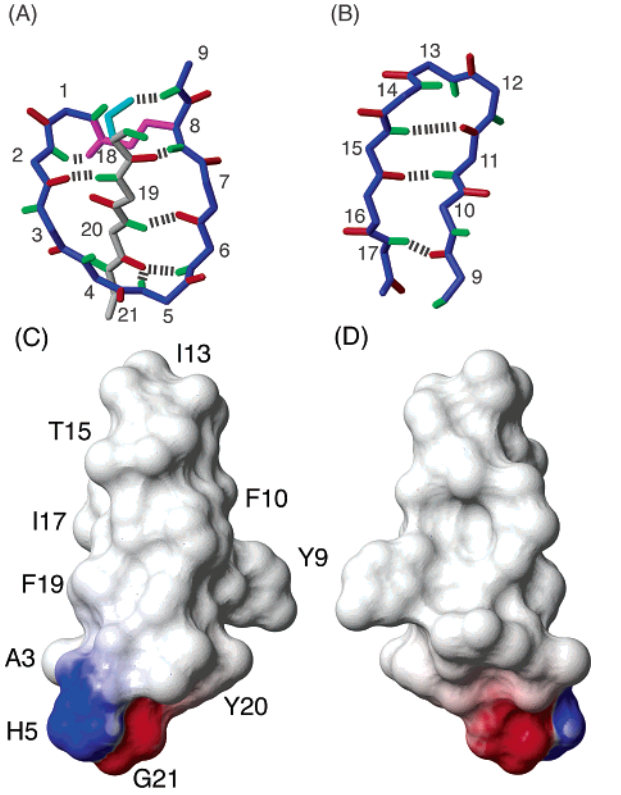

Figure 8. Hydrogen bond network and electrostatic surface of MccJ25. The hydrogen bonds identified from the structures of MccJ25 reported here and the slow exchange amides reported by Blond et al.[25] are highlighted by dashed lines. View (A) illustrates hydrogen bonds in sheet A and the ring structure whereas view (B) shows interactions in sheet B and the β-hairpin. Amide protons and carbonyls are shown in green and red, respectively. The Gly1-Glu8 link is shown in magenta and the side chain of Ser18 is shown in cyan. MccJ25 is highly hydrophobic and carries only two charges, His5 and the C-terminus, which appear to be interacting closely possibly in the form of a salt bridge (panels C and C). Blue and red represent positive and negative charge, respectively. Selected amino acids are labeled with residue number and single letter amino acid codes. View (D) is rotated 90° in relation to (C).

by endoprotease GluC. In addition MccJ25 retained its structured core when digested by thermolysin. Although such an observation seems unlikely for a 21 amino acid peptide without cross-bracing disulfides or alternative linkages, it is perfectly consistent with MccJ25 having a backbone-to-side chain linkage and a threaded structure. Thermolysin hydrolyzes the Phe10-Val11 bond and the cleaved form was shown to have significantly decreased antimicrobial activity.[11] This region is directly involved in the β-hairpin comprising β-strands between residues 10−11 and 15−16 and a β-turn involving residues 11−14. Thus, digestion with thermolysin would have major implications for the secondary structure in this region but not necessarily for the N-terminal part of the molecule. These results imply that the β-hairpin may have a significant role in the antimicrobial activity. In particular, it is interesting to note that studies indicate that the enzymatically linearized material does retain some activity against *S. newport*, suggesting that the hairpin might be more important for the enzyme inhibition of RNA polymerase in *E. coli* than for the less specific membrane interactions that have been reported for *S. newport*.

Mass spectrometry analysis indicates that the residues threaded through the ring stay associated after breakage of the peptide chain, even during the harsh conditions experienced in the mass spectrometer. Although this stability initially prompted us to consider the possibility of a second internal covalent linkage, no MS data could be found to support the presence of additional cross bracing. Instead the structural data generated by NMR provided an explanation. From Figure 7 it is clear that the ring structure wraps tightly around the C-terminus and there are a number of interactions between these parts of the molecule, including the small β-sheet involving residues 6−8 and 18−20. Although these interactions alone might account for a high stability, the presence of the bulky aromatic side chains of Phe19 and Tyr20 on each side of the ring appears to make it virtually impossible to unthread the C-terminal tail without breaking the ring or the Phe19-Tyr20 peptide bond.

The revised three-dimensional structure of MccJ25 is also more consistent with the slow exchange NMR data than the originally proposed structure. Blond et al.[25] reported that a large number of amide protons showed slow exchange with D_2O solvent, which is consistent with a tight fold stabilized by an extensive network of hydrogen bonds. However, in the reported model several of the slow exchanging amides did not appear to be involved in hydrogen bonds. By contrast, the threaded model accounts for hydrogen bonds for all but one of the medium and slow exchanging amides. It is interesting to note that the sole exception, Phe10, has an amide temperature coefficient of 9 ppb/K, which strongly suggests that it is not involved in a hydrogen bond.[41] On the other hand the amide temperature coefficient of His5 (−2.4 ppb/K) does suggest that it is involved in a hydrogen bond, despite the fast exchange behavior of the amide proton. This is supported by the structure, which reveals that this amide is in close proximity to the carbonyl of Tyr20. Figure 8 (panels A and B) shows the backbone heavy atoms and amide protons of the lowest energy structure of MccJ25 and illustrates the entire network of suggested hydrogen bonds.

(41) Cierpicki, T.; Otlewski, J. *J. Biomol. NMR.* **2001**, *21*, 249−261.

MccJ25 carries only two charges, namely His5 and the C-terminus, once the Glu is sequestered in the internal linkage. It is interesting to note that these are close in the three-dimensional structure and that an interaction between them might provide further stability to the fold. The electrostatic surface potential of MccJ25 (Figure 8, panels C and D) illustrates this apparent interaction between the two charges and highlights the highly hydrophobic nature of this molecule overall. Interestingly a recent report chemically modified the charged residues of MccJ25 and noted a significantly decreased activity.[42] The authors of this study based their discussion on the reported macrocyclic structure and thus believed that the modification achieved involved the Glu8 side chain. However, as we have shown here the only free carboxyl group in MccJ25 is the C-terminus and thus we conclude that the modification must have involved this group. Nonetheless, it is interesting to note that the charges are crucial for the antimicrobial action of MccJ25.

Alhtough the proposed threaded noose is a fascinating structural motif, the discovery of a side chain-to-backbone linkage in MccJ25 is perhaps not surprising given that several other bacterial proteins of a similar size contain such a linkage. Indeed, a backbone head-to-tail cyclized form may be regarded as a break from precedent as the known backbone cyclized bacterial proteins are generally larger.[16] In the early 1990s, two peptides, an atrial natriuretic peptide, anantin,[43] and an inhibitor of prolyl endopeptidase, propeptin,[44] were isolated from bacteria and shown to contain linkages between the N-terminal Gly residues and the side chains of Asp residues at positions 8 and 9, respectively. Additional peptides containing a similar linkage have subsequently been discovered, including RES-701-1,[45] MS-271[46] and RP71955,[47] all of which have been isolated from *Streptomyces* species. However, it should be noted that peptides containing this linkage are not restricted to *Streptomyces* species, as propeptin is isolated from *Microbispora* and MccJ25 is isolated from *E. coli*. Despite the conserved backbone-to-side chain linkage, some of these peptides, including MS-271 and RP71955, contain disulfide bonds whereas anantin, propeptin and RES-701-1 do not. There is very little sequence similarly across these peptides, however they all possess a large number of aromatic residues and are hydrophobic in nature.

The three-dimensional structures have been determined for several of these bacterial peptides and revealed a similar structural motif to the revised structure of MccJ25 in which the C-terminal is threaded through the ring formed by the backbone-to-side chain linkage. A comparison of the structure of RP71955 and MccJ25 is shown in Figure 9.[47−49] This conformation has been described as a "lasso" type structure.[48]

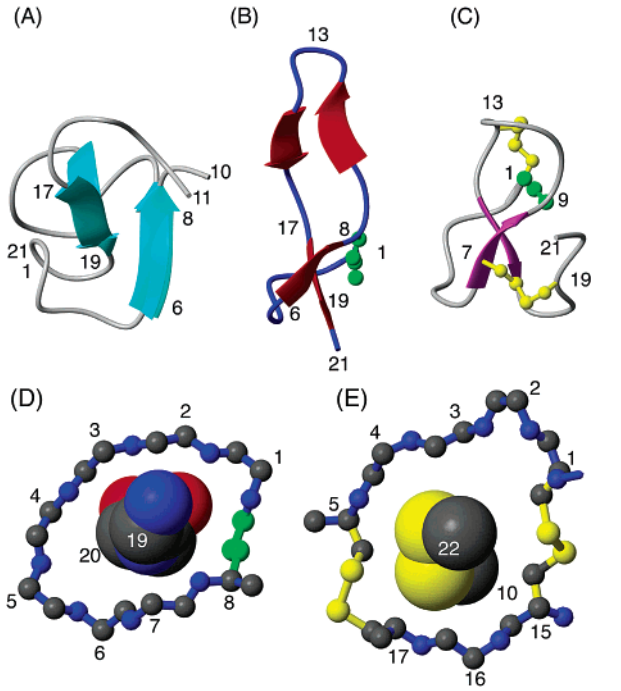

Figure 9. Comparison of the published macrocyclic structures of native and thermolysin linearized MccJ25 (A), the structure derived in this study (B) and RP71955 (C). All structures are shown in ribbon style with the backbone-side chain link in green and disulfide bonds in yellow ball-and-stick representations. It is clear that the proposed β-sheet in the macrocyclic MccJ25 is indeed present and is further stabilized by the Gly1-Glu8 link. This link also fully accounts for the behavior and stability of the structured core of the thermolysin linearized analogue. The threading of the C-terminus in MccJ25 is also observed in RP71955. Although the C-terminal is threaded further through the ring in RP71955, the core and the β-sheet comprising one strand from the ring and one strand from the penetrating peptide backbone are similar for both structures. In the case of RP71955, the ring comprises one additional residue but the structure is further stabilized by the two disulfide bonds. Panels (D and E) show a comparison of the threaded arrangement in MccJ25 and kalata B1. In MccJ25 the ring is formed by the backbone of residues 1−8 and the N-terminus to Glu8 side chain link while in kalata B1 the ring comprises the backbone of residues 1−5 and residues 15−17 together with the disulfides 1−15 and 5−17. The penetrating segment (the peptide chain in MccJ25 and the 10−22 disulfide in kalata B1) is shown in a spacefilling model to illustrate the remarkably tight fit.

In studies consistent with our studies on MccJ25 a synthetic form of RES-701-1 was shown to be completely different to the native form in terms of activity and structure despite containing an identical primary structure. Katahira et al.[49] suggested that it is impossible for the tail to thread through the ring after it is formed, and thus the ring must be closed after appropriate folding and may involve an enzymatic reaction. This hypothesis fits very well with the MccJ25 data as the structure suggests that the tail cannot unthread and indeed even after fragmentation it appears the tail remains in the ring and behaves as one entity during MS/MS.

The tightly folded structure of MccJ25 is likely to have played a role in the development of the original hypothesis that the peptide is backbone cyclized. As evident from Figure 9, the suggested macrocylic structure does have some similarities to the threaded structure i.e., the β-sheet and the tight fold in the region around the termini. Edman degradation and carboxypeptidase Y cleavage suggested the presence of blocked N and C-termini.[11] Our current study provides an explanation for both these observations, as the N-terminal is indeed blocked and the three-dimensional structure suggests that the C-terminus is

(42) Bellomio, A.; Rintoul, M. R.; Morero, R. D. *Biochem. Biophys. Res. Commun.* **2003**, *303*, 458−462.
(43) Wyss, D. F.; Lahm, H. W.; Manneberg, M.; Labhardt, A. M. *J. Antibiot. (Tokyo)* **1991**, *44*, 172−180.
(44) Ezumi, Y.; Itoh; Uramoto, M.; Kimura, K.; Gotou, M.; Yoshihama, M. *Nippon Nogeikagaku Kaishi* **1992**, 460.
(45) Morishita, Y.; Chiba, S.; Tsukuda, E.; Tanaka, T.; Ogawa, T.; Yamasaki, M.; Yoshida, M.; Kawamoto, I.; Matsuda, Y. *J. Antibiot. (Tokyo)* **1994**, *47*, 269−275.
(46) Yano, K.; Toki, S.; Nakanishi, S.; Ochiai, K.; Ando, K.; Yoshida, M.; Matsuda, Y.; Yamasaki, M. *Bioorg. Med. Chem.* **1996**, *4*, 115−120.
(47) Frechet, D.; Guitton, J. D.; Herman, F.; Faucher, D.; Helynck, G.; Monegier du Sorbier, B.; Ridoux, J. P.; James-Surcouf, E.; Vuilhorgne, M. *Biochemistry* **1994**, *33*, 42−50.
(48) Katahira, R.; Yamasaki, M.; Matsuda, Y.; Yoshida, M. *Bioorg. Med. Chem.* **1996**, *4*, 121−129.
(49) Katahira, R.; Shibata, K.; Yamasaki, M.; Matsuda, Y.; Yoshida, M. *Bioorg. Med. Chem.* **1995**, *3*, 1273−1280.

sufficiently inaccessible for enzyme degradation. The strongest evidence for the macrocyclic structure in the original study came from manual Edman sequencing.[11] In particular, one fragment obtained from thermolysin cleavage of MccJ25 was reported to overlap the N- and C-termini, i.e., Gly21 to Gly1. However, considering the unambiguous evidence of a free C-terminal in this study, a plausible explanation to this observation might be a carry over effect of the C-terminal Gly21. This seems likely, as three out of the four residues reported in the N-terminal continuation of the sequence are Gly residues, including Gly1-Gly2.

On the basis of the suggested macrocyclic fold Blond et al. commented on general similarities between MccJ25 and the cyclotide kalata B1. When considering our revised structure the overall folds of these molecules have little in common. However, interestingly, both structures comprise an embedded ring penetrated by another part of the molecule. In kalata, a disulfide penetrates a ring formed by two other disulfide bonds and their interconnecting backbones, giving rise to a so-called cystine knot motif. Studies in our laboratory have shown that the cystine knot is absolutely crucial for the folding and stability of kalata B1.[50] Similarly, it appears the threaded structure in MccJ25 is responsible for the exceptional stability. From Figure 9, panels (D and E), which show the "knotted" arrangements of MccJ25 and kalata B1, it is clear that the "ring" in MccJ25 comprises two less atoms and thus wraps even tighter around the penetrating peptide chain.

In summary, we have shown that MccJ25 is not backbone cyclic but belongs to a family of bacterial proteins containing internal linkages between the N-terminus and the side chain of an Asp or Glu residue. Bacterial proteins containing such linkages have been shown to exhibit resistance to protease digestion, suggesting that this "lasso" structure may be present to provide stability to otherwise small, and in the case of those not containing disulfide bonds, unconstrained peptides. On the basis of the three-dimensional structure this linkage is likely to occur after appropriate folding and it appears that some chaperone-like folding mechanism may be required to maintain the structure prior to formation of the internal linkage. This might involve either facilitation from the leader sequence in the precursor protein for MccJ25, or an external chaperone, or both. The structural findings reported here are consistent with an independent study by Wilson et al. reported in the same issue of this journal.[51]

Acknowledgment. We thank Dr. Sylvie Rebuffat for supplying a sample of native MccJ25 and Dr. Tom Muir and Dr. Phil Dawson for helpful discussions. D.J.C. is an Australian Research Council (ARC) Professorial Fellow. We thank the A.R.C. for grant support for this work.

Supporting Information Available: Table SI listing MS/MS fragments observed for native and macrocyclic MccJ25. This material is available free of charge via the Internet at http://pubs.acs.org.

JA0367703

(50) Daly, N. L.; Craik, D. J. *J. Biol. Chem.* **2000**, *275*, 19 068−19 075.

(51) Wilson, K.-A.; Kalkum, M.; Ottesen, J.; Yuzenkova, J.; Chait, B. T.; Landick, R.; Muir, T.; Severinov, K.; Darst, S. *J. Am. Chem. Soc*. **2003**, 125, 12475−12483.